Original Paper

Pathobiology

Pathobiology 2007;74:336–343
DOI: 10.1159/000110027

Received: April 12, 2007
Accepted after revsion: July 19, 2007

Inducible Nitric Oxide Synthase Mediates Hypoxia-Induced Hypoxia-Inducible Factor-1α Activation and Vascular Endothelial Growth Factor Expression in Oxygen-Induced Retinopathy

Tao He Ming Ai Xiao-Hui Zhao Yi-Qiao Xing

Department of Ophthalmology, Renmin Hospital of Wuhan University, Wuhan, China

Key Words

Inducible nitric oxide synthase · Hypoxia-inducible factor-1α · Phosphatidylinositol 3-kinase/Akt · Vascular endothelial growth factor · Oxygen-induced retinopathy

Abstract

Objective: Previous studies provided evidence that many factors contribute to retinal angiogenesis, including inducible nitric oxide synthase (iNOS), hypoxia-inducible factor-1α (HIF-1α) and vascular endothelial growth factor (VEGF). But the role of nitric oxide generated by iNOS in the regulation of expression of hypoxia-inducible genes in retinopathy of prematurity remains unclear. So we sought to better define the molecular basis of this iNOS-dependent regulation. ***Methods:*** In this study, using immunohistochemistry, real-time PCR and Western blotting technologies, we investigated the changes of iNOS, HIF-1α, VEGF and phosphatidylinositol 3-kinase/Akt (PI3K/Akt) expressions. ***Results:*** Hypoxia-induced overexpression of iNOS, HIF-1α, VEGF, PI3K/Akt and phosphorylated PI3K/Akt was observed in the untreated retinopathy of the prematurity group. Administration of the selective iNOS inhibitor aminoguanidine hemisulfate markedly decreased the expression of these genes. ***Conclusions:*** These results indicate that iNOS mediates HIF-1α activation and VEGF expression in retinal angiogenesis and that the PI3K/Akt signaling pathway may play a role in this process.

Introduction

Retinopathy of prematurity (ROP) is an important cause of preventable blindness in children. It is a vasoproliferative disorder of the retina primarily affecting severely premature infants. Administration of high concentration of oxygen (the main risk factor of ROP) is an important treatment for extremely low birth weight neonates; under this condition, hyperoxia leads to the generation of reactive oxygen species [1] and thus cause cellular injury and the breakdown of retinal capillary network. During following normoxia (relative hypoxia), the overexpression of vasoactive substances causes the development of retinal neovascularization. Recent reports suggest that reactive oxygen species play an important role in angiogenesis, however, its underlying molecular mechanisms remain unknown [2].

Hypoxia is an important regulatory stimulus for diverse biological processes such as angiogenesis [3]. The molecular mechanisms which control hypoxia-induced gene expression have been extensively studied. Under low oxygen, a variety of cells produce many vasoactive substances, including vascular endothelial growth factor (VEGF) [4], and ultimately lead to the formation of retinal neovascular. Expression of these genes is regulated by hypoxia-inducible factor-1α (HIF-1α), a transcription factor whose levels are tightly regulated by oxygen levels.

KARGER

Fax +41 61 306 12 34
E-Mail karger@karger.ch
www.karger.com

1015–2008/07/0746–0336$23.50/0

Accessible online at:
www.karger.com/pat

Dr. Yi-Qiao Xing
Department of Ophthalmology
Renmin Hospital of Wuhan University, 238 Jiefang Road
Wuhan, Hubei Province 430060 (China)
Tel. +86 27 6327 4696, Fax +86 27 8804 2292, E-Mail xyqdr07@yahoo.com.cn

Under normoxic conditions, HIF-1α is ubiquitinated and proteosomally degraded. During hypoxia, HIF-1α escapes the ubiquitination/degradation and rapidly accumulates in the cell nucleus along with its heterodimer partner HIF-1β, and then it binds to a hypoxia-response element, thus activating hypoxia-sensitive genes [5]. Although the molecular characterization of the HIF-1 complex has been performed, signaling mechanisms regulating HIF-1α protein expression remain to be studied.

Nitric oxide (NO) is an important signaling molecule that mediates a variety of essential physiological processes, NO generated by the inducible NO synthase (iNOS) has been implicated in many hypoxic diseases [6]. In the eye, it has been reported that NO plays a role in glaucoma, diabetic retinopathy and ischemic retinopathy [7]. It has been shown that upregulated expression of HIF-1α, iNOS and VEGF in the retina was observed in response to hypoxia [4]. In contrast, few data exist on the relationship between HIF-1α and its downstream genes such as iNOS and VEGF in ROP.

Phosphatidylinositol 3-kinase (PI3K) is a heterodimeric enzyme composed of a catalytic and a regulatory subunit. The best-known downstream target of PI3K is the serine-threonine kinase Akt, which transmits survival signals from growth factors. Growth factors, cytokines and other signaling molecules can stimulate HIF-1α protein synthesis via activation of the PI3K/Akt pathways. Evidence suggests that PI3K is important in the process of PGE2-stimulated VEGF expression in cancer [8]. So we speculated that the PI3K/Akt signaling pathway was correlated with VEGF and HIF-1α expression and retinal angiogenesis regulated by iNOS in mouse model of ROP.

In the present study, using an oxygen-induced retinopathy (OIR) mouse model, we investigated the expression of HIF-1α, iNOS and VEGF in the retinas of experimental animals. Moreover, we studied the effect of iNOS inhibition on HIF-1α and VEGF expression, and the changes of PI3K/Akt signaling in this process.

Materials and Methods

Animal Model and Treatment

Pregnant female C57BL/6J mice were provided by the Laboratory Animal Center of Wuhan University. All experiments were conducted in accordance with the Animal Care and Use Committee and the Association for Research in Vision and Ophthalmology Statement for the Use of Animals in Ophthalmic and Vision Research.

This mouse model of oxygen-induced retinopathy was first described by Smith et al. [9]. OIR was induced in C57BL/6J mice by placing 7-day-old pups with their mothers in an oxygen-regulated chamber under hyperoxic conditions (75 ± 5% O_2). Gas levels in the chamber were monitored every 8 h with a gas analyzer (model CY-12C; Electrochemical Analytical Instruments Ltd., Meicheng, China) and recorded. Mice remained in the chamber for 5 days (hyperoxic period, postnatal day (P)7–P12) and were then removed and kept under normoxic conditions for a further 5 days (relative hypoxia-induced angiogenesis, P12–P17).

The mothers were randomly divided into 3 experimental groups with 14 pups per group. Group 1 was the normal group, group 2 consisted of untreated ROP animals and group 3 included the ROP animals treated with aminoguanidine hemisulfate (Sigma), the selective iNOS inhibitor. In the normal group, the mother and her newborn pups were housed in room air from P0 to P17. In the untreated ROP group, ROP was induced in C57BL/6J pups. In the ROP treated with aminoguanidine hemisulfate group, the OIR induction protocol was used and the mice were treated with aminoguanidine hemisulfate (100 mg/kg body weigh, intraperitoneally) [10–12] daily from P12 until P17.

During the experiment, mothers were provided with water and standard mice chow ad libitum and exposed to normal 12-hour light-dark cycles. Pups received nutrition from their mothers.

Histopathology and Immunohistochemistry

After the 17-day experimental period, the 17-day-old mice were sacrificed by an intraperitoneal injection of pentobarbital (120 mg/kg body weight; Boster, Wuhan, China). Eyeballs (n = 12) were removed from animals and fixed for 6 h in formalin fixative. The fixed eyes were dehydrated through ascending concentrations of alcohol before being embedded in paraffin wax, serially sectioned at 3 μm and placed on poly-L-lysine-coated slides. Sections were collected and incubated overnight at 37°C. A standard staining procedure with hematoxylin and eosin was performed. In addition, immunohistochemical staining was performed. Randomly chosen eye sections were deparaffinized and incubated for 10 min with 3% hydrogen peroxide and then incubated for 20 min at room temperature with normal goat serum, diluted 1:10 with 0.1 M phosphate-buffered saline (PBS, pH 7.4). The sections were then incubated overnight at 4°C with HIF-1α, iNOS, VEGF rabbit polyclonal antibody and cluster of differentiation 34 (CD34) goat polyclonal antibody (all from Santa Cruz; 1:200 in PBS). All sections were then washed with 0.1 M PBS (three 2-min washes) to reduce nonspecific binding. After this, sections were incubated with biotinylated goat anti-rabbit or rabbit anti-goat IgG (Boster, China; 1:200 in PBS) for 20 min at room temperature. The sections were then rinsed with 0.1 M PBS (three 2-min washes) and reacted with streptavidin-biotin peroxidase complex (Boster). After three 4-min washes with 0.1 M PBS, sections were stained with 0.05% diaminobenzidine (Sigma) for 1 min before rinsing in tap water for 5 min. The sections were then stained with Mayer hematoxylin, differentiated in Scott tap water, dehydrated in alcohol, cleared in a paraffin solvent and clearing agent, and mounted in dibutyl phthalate xylene. Negative control specimens were obtained by staining without the primary antibodies. The positive cells and the distribution of positively stained tissue areas were analyzed in the sections per high-power field (×400). The num-

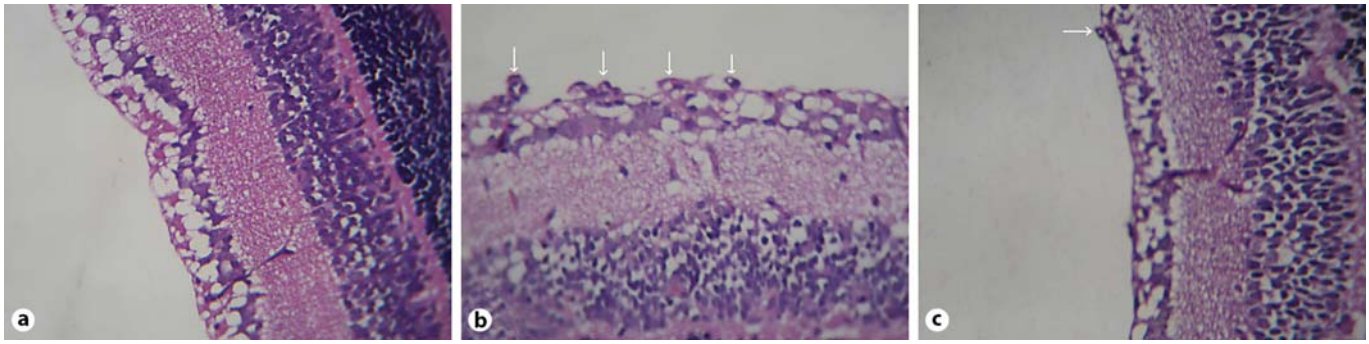

Fig. 1. Histopathology of the inner retina of C57BL/6J mice. Sections are counterstained with Mayer hematoxylin and eosin. **a** Normal group. **b** Untreated ROP group. **c** ROP treated with aminoguanidine hemisulfate group. Arrows represent blood vessels protruding into the vitreous. ×400.

ber of cell nuclei of preretinal neovascular endothelial cells was counted too. All readings were done independently by 2 observers in a masked fashion.

RNA Extraction and Real-Time PCR

Eyeballs were enucleated from the mice at P17. Retinas were separated from eyeballs (n = 8) on an iced plate and immediately frozen in liquid nitrogen until further use. Total RNA was extracted from the frozen retina tissues using Trizol reagent according to the manufacturer's instructions. The total RNA concentrations from each group were determined by measuring the optical density at 260 and 280 nm using an ultraviolet light spectrophotometer. Aliquots of 20 μl RNA from each group were applied for production of cDNA. One microliter of cDNA from each group was amplified in 25 μl of reactive mixture with 0.25× SYBR Green Supermix (Molecular Probes). Quantitative PCR was performed by monitoring in real time the increase in fluorescence of SYBR Green using Rotor-Gene 3000 Real-time PCR (Corbett Research). The primer sequences were as follows: iNOS: 5′-GGC AGC CTG TGA GAC CTT TG-3′, 5′-GCA TTG GAA GTG AAG CGT TTC-3′; HIF-1α: 5′-AGT CCC ATG AAG TGA TCA AGT TCA-3′, 5′-ATC CGC ATG ATC TGC ATG G-3′; VEGF: 5′-TTA CTG CTG TAC CTC CAC CA-3′, 5′-ATG TAG AAG TTC GGC AGG ACA-3′. The thermal cycling program consisted of 5 min at 95°C, 35 cycles of 10 s at 95°C, 15 s at 58°C and 20 s at 72°C. After the completion of each extension step (72°C), the fluorescence of each sample was measured at 81°C to exclude any possible nonspecific reactions. Cycle threshold values were determined by automated threshold analysis. No amplification was detected in negative controls (real-time PCR without reverse transcriptase, or samples with H_2O instead of cDNA). Primer quality (lack of primer-dimer amplification) was confirmed by melting curve analysis. Relative quantitation of the gene expression was performed using the standard curve method. All experiments were carried out in triplicate. For each sample the mean ± SEM of the relative amount of mRNA was normalized to the mean of GAPDH.

Western Blot Analysis

Retinas were separated from eyeballs (n = 8) of each group on an iced plate and immediately frozen in liquid nitrogen until further use. The retinas were lysed for 10 min at 4°C in 200 μl of lysis buffer (20 mM Tris, pH 7.4; 150 mM NaCl; 1 mM ethylenediamine tetraacetic acid; 1 mM orthovanadate; 1 mM phenylmethylsulfonyl fluoride; 1 μg/ml leupeptin; 10 μg/ml aprotinin). After homogenization and centrifugation, the supernatant was collected for total protein values. The amount of protein was determined with the BCA protein assay kit (Sigma).

Forty micrograms of protein from each sample was loaded on sodium dodecyl sulfoxide polyacrylamide gel electrophoresis (SDS-PAGE) and then proteins were transferred to a nitrocellulose membrane (Hybond-C; Amersham, Arlington Heights, Ill., USA) at 200 mA for 1 h. Antibody reaction was performed after blocking of nonspecific binding sites with 5% skim milk. The membrane was incubated with the primary antibodies overnight at 4°C: iNOS (1:500 in PBS; Santa Cruz), HIF-1α (1:500 in PBS; Santa Cruz), PI3K (1:500 in PBS; Santa Cruz), Akt (1:500 in PBS; Santa Cruz) and VEGF (1:500 in PBS; Santa Cruz); activation of PI3K and Akt was examined using specific phosphorylated antibodies (1:1,000 in PBS; Cell Signaling Technology). Then, membranes were washed with TBS and incubated with horseradish peroxidase-conjugated secondary antibody (goat anti-rabbit antibody; Boster) in blocking buffer for 2 h at room temperature. After 3 washes, the proteins were visualized with enhanced chemiluminescence (Amersham) detection. β-Actin was served as loading control. Experiments were repeated 3 times.

Statistical Analysis

All values were given as means ± SEM. Statistical analysis was performed with Student's t test. $p < 0.05$ were considered statistically significant.

Results

Histopathology and CD34 Immunostaining

In the normal group, the vasculature of the inner retina appeared normal, with blood vessels confined to the inner retina (fig. 1a, 2a). In contrast, in the untreated ROP group, large and conglomerate new blood vessels

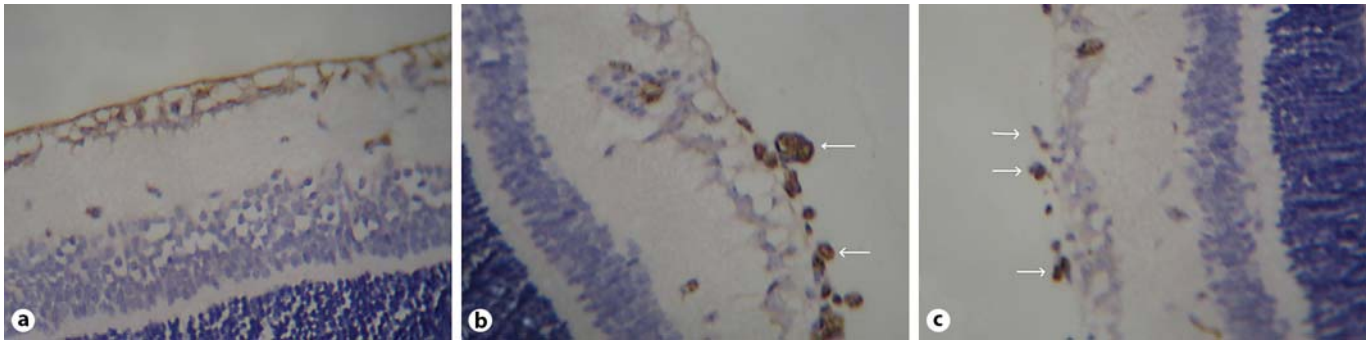

Fig. 2. CD34 immunostaining in 3-μm paraffin-embedded sections of retina from C57BL/6J mice. **a** Normal group. **b** Untreated ROP group. **c** ROP treated with aminoguanidine hemisulfate group. Arrows represent CD34 immunolabeling expressed in endothelial cells. ×400.

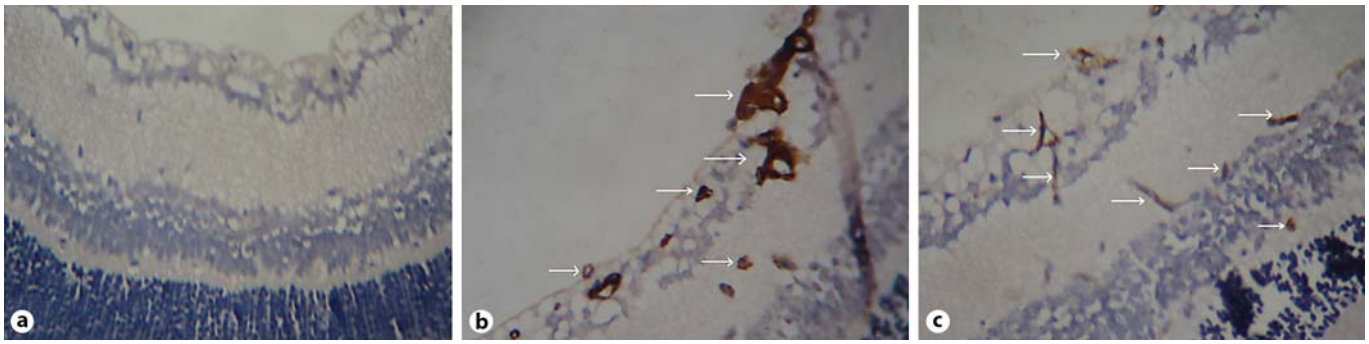

Fig. 3. Immunolabeling for iNOS in 3-μm paraffin-embedded sections of retina from C57BL/6J mice. **a** Normal group. **b** Untreated ROP group. **c** ROP treated with aminoguanidine hemi-sulfate group. Arrows represent iNOS immunolabeling expressed in cells and blood vessels. ×400.

adherent to the internal limiting membrane were observed in 100% of specimens (fig. 1b, 2b). In the ROP treated with aminoguanidine hemisulfate group, the administration reduced these lesions by 33.3%, the new blood vessels appeared small and sparse (neovascular nuclei count: normal group 0.28 ± 0.06; untreated ROP group 47.58 ± 15.94; ROP treated with aminoguanidine hemisulfate group 35.96 ± 8.94; $p < 0.001$; fig. 1c, 2c).

Immunohistochemistry

In the normal group, there is no detectable level of iNOS expressed in the inner retina (fig. 3a). In the untreated ROP group, iNOS expression was significantly increased in the inner nuclear layer, inner and outer plexiform layers, especially in the endothelial cells of new blood vessels (fig. 3b). In the ROP treated with aminoguanidine hemisulfate group, the staining of iNOS was weaker than in the untreated ROP group (fig. 3c).

There is no detectable level of HIF-1α expressed in the retina of the normal group (fig. 4a). In contrast, the HIF-1α immunoreactivity was strong in the retina of the untreated ROP group, most prominently in highly vascularized lesions (fig. 4b). In the ROP treated with aminoguanidine hemisulfate group, specific HIF-1α immunolabeling was attenuated, compared with the untreated ROP group (fig. 4c).

Only weak staining for VEGF was present in the inner retina in the normal group (fig. 5a). Conversely, strong VEGF staining was detected in untreated ROP mice, especially in the retinal vessels and also in the vessels protruding in vitreous cavity (fig. 5b). In the ROP treated with aminoguanidine hemisulfate group, the immunolabeling for VEGF was attenuated (fig. 5c).

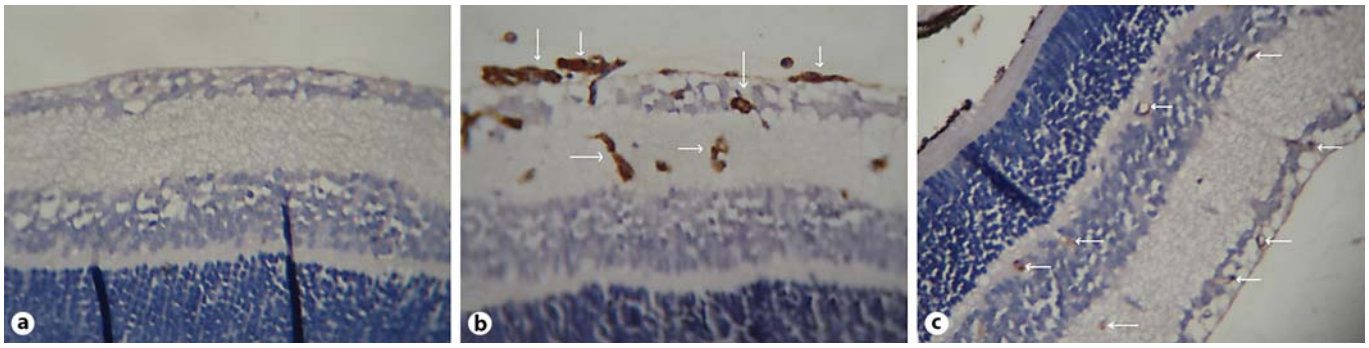

Fig. 4. Immunolabeling for HIF-1α in 3-μm paraffin-embedded sections of retina from C57BL/6J mice. **a** Normal group. **b** Untreated ROP group. **c** ROP treated with aminoguanidine hemi-sulfate group. Arrows represent HIF-1α immunolabeling expressed in cells and blood vessels. ×400.

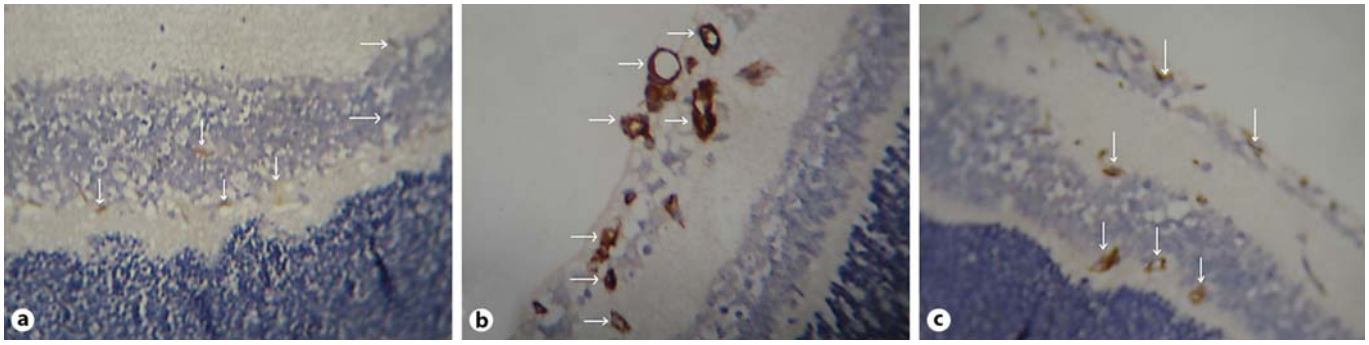

Fig. 5. Immunolabeling for VEGF in 3-μm paraffin-embedded sections of retina from C57BL/6J mice. **a** Normal group. **b** Untreated ROP group. **c** ROP treated with aminoguanidine hemi-sulfate group. Arrows represent VEGF immunolabeling expressed in cells and blood vessels. ×400.

mRNA Expression of HIF-1α, iNOS and VEGF by Real-Time PCR

Real-time PCR analysis was performed to assess the mRNA levels of HIF-1α, iNOS and VEGF in the retinas of experimental animals. As shown in figure 6, hypoxia-induced overexpression of HIF-1α, iNOS and VEGF was observed in the untreated ROP group, the administration of aminoguanidine hemisulfate significantly inhibited the mRNA expression of these genes.

The iNOS mRNA level in the untreated ROP group was more than 11 times higher than in the normal group and about 2.1 times higher than in the ROP treated with aminoguanidine hemisulfate group ($p < 0.01$). The HIF-1α mRNA level in the untreated ROP group was about 7.4 times higher than in the normal group and about 1.6 times higher than in the ROP treated with aminoguanidine hemisulfate group ($p < 0.01$). The VEGF mRNA level in the untreated ROP group was about 2.9 times higher than in the normal group and about 1.3 times higher than in the ROP treated with aminoguanidine hemisulfate group ($p < 0.01$).

Protein Expression of HIF-1α, iNOS, VEGF, PI3K/Akt and Phosphorylated PI3K/Akt by Western Blot Analysis

The protein expression of HIF-1α, iNOS, VEGF, PI3K/Akt and phosphorylated PI3K/Akt in retina specimens from the 3 groups was studied using a Western blot technique (fig. 7).

In the normal group, the protein expression of HIF-1α and iNOS was almost impossible to detect, however, the expression of PI3K, Akt and VEGF was relatively strong. As for the untreated ROP group, the expression of these proteins was significantly increased ($p < 0.05$, untreated

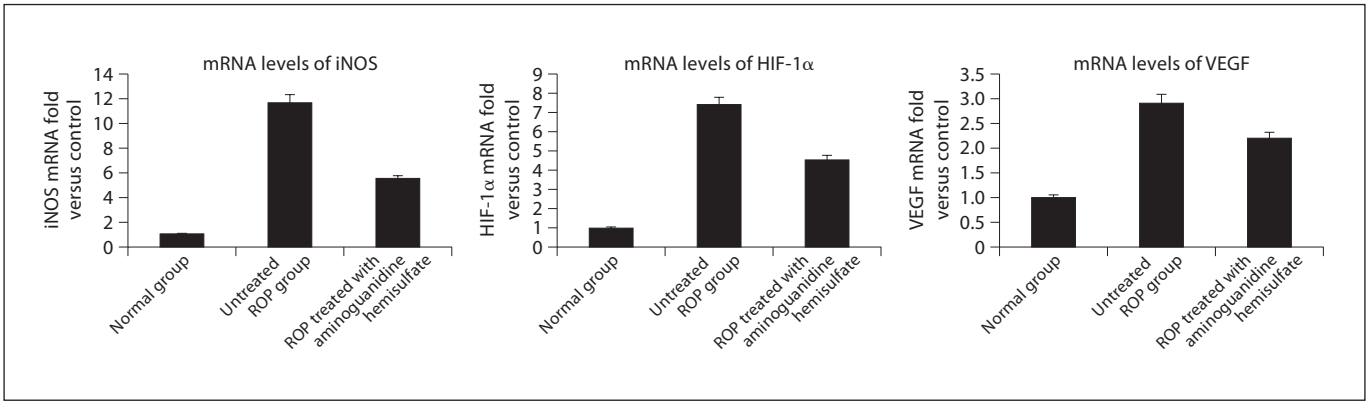

Fig. 6. Relative amount of iNOS, HIF-1α and VEGF mRNA in 3 groups measured by quantitative real-time PCR. Means ± SEM of mRNA level normalized to GAPDH (internal control) were calculated. Statistical significance was determined by Student's t test ($p < 0.05$).

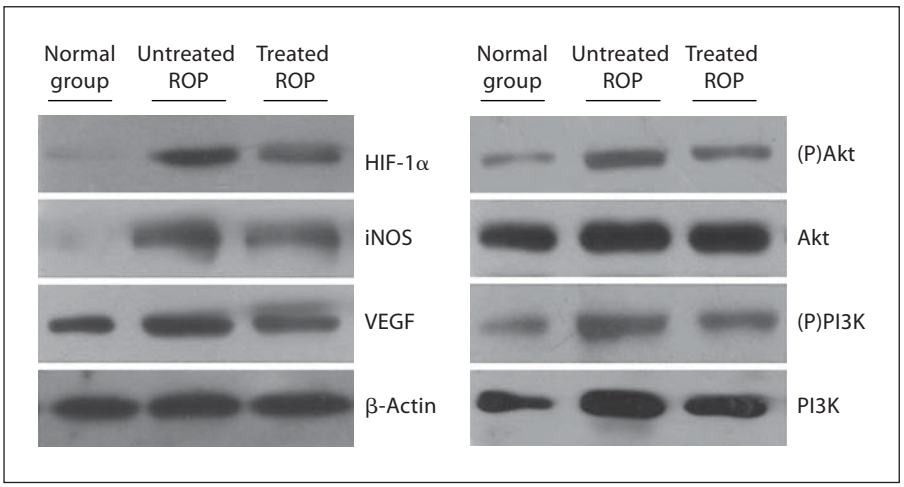

Fig. 7. Western blot analysis for HIF-1α, iNOS, VEGF, PI3K/Akt and phosphorylated PI3K/Akt in the retinas of experimental animals. The bands of protein expression were measured by densitometry with Quantity One quantitation analysis software package. The protein expression levels were elevated markedly in the untreated ROP group compared with the normal group. After the administration of aminoguanidine hemisulfate, the expression of these proteins was significantly suppressed compared with the untreated ROP group, but still stronger than in the normal group. Statistical significance was determined by Student's t test ($p < 0.05$).

ROP group compared with normal group), especially of HIF-1α and iNOS. The expression of these proteins was markedly suppressed by the administration of aminoguanidine hemisulfate ($p < 0.05$, untreated ROP group compared with ROP treated with aminoguanidine hemisulfate group), but remained stronger than in the normal group ($p < 0.05$, normal group compared with ROP treated with aminoguanidine hemisulfate group).

In addition, Western blot analysis of phosphorylated PI3K and Akt showed that the oxygen treatment resulted in a significant increase in phosphoryleted PI3K and Akt levels in the untreated ROP group, and the administration of aminoguanidine did indeed attenuate PIk and Akt phosphorylation.

Discussion

It is well known that HIF-1α plays an important role in hypoxia-induced diseases. However, few experimental studies have explored the role of HIF-1α in ROP. Using engineered mouse models, Morita at al. [13] and Brafman et al. [14] evidenced that HIF play a role in hypoxia-induced retinal angiogenesis. Another study [4] demonstrated that the expression of HIF-1α was observed in retina after hypoxia. In our study, hypoxia-induced HIF-1α overexpression was observed in the untreated ROP group. Along with suppressed expression of HIF-1α, retinal angiogenesis reduction was also observed. These results indicate that HIF-1α must play an important role in ROP.

As is well known, HIF-1α can mediate iNOS expression under hypoxia condition. On the other hand, previous studies revealed that NO is a key factor sustaining HIF-1α activation during hypoxia [15–17]. Furthermore, NO has been reported both to promote and to inhibit the activity of HIF-1 [15, 16, 18]. But the role of NO generated by iNOS in the regulation of expression of hypoxia-inducible genes in ROP remains unclear. In the present study, increased mRNA and protein expression of iNOS, HIF-1α and VEGF was observed in the untreated ROP group. The administration of the selective iNOS inhibitor aminoguanidine hemisulfate markedly decreased these expressions, and resulted in reduced angiogenesis. So we speculated that excess production of NO generated from iNOS plays an important pathogenic role in hypoxia-induced retinal damage. This result suggested that iNOS inhibition not only decreased HIF-1α expression but also lowered VEGF expression, and that there must be an interactive mechanism between the HIF-1α and iNOS cascade.

A previous study showed that hypoxia-induced iNOS expression in microglia is regulated by HIF-1α via a PI3K/Akt-dependent pathway [19]. Other findings revealed that the PI3K/Akt signaling pathway can mediate the expression of HIF-1α [20–22]. Recognizing which signal transduction pathway is active in hypoxia-induced retinal angiogenesis may be an important information and may identify a potential target for antiangiogenic therapy. In our study, hypoxia-induced PI3K/Akt activation was observed in the untreated ROP group. The administration of the selective iNOS inhibitor aminoguanidine hemisulfate significantly suppressed the activation of PI3K/Akt proteins. Our results pointed to the important role of the PI3K/Akt pathway in the modulation of iNOS effect on HIF-1α and VEGF expressions, and corroborated earlier observations on the involvement of the PI3K/Akt signaling pathway in affecting HIF-1α protein appearance.

In conclusion, we showed in this paper that the iNOS inhibition can downregulate both VEGF and HIF-1α and can thus decrease retinal angiogenesis. We presume that the mechanism by which the iNOS inhibition downregulates VEGF and HIF-1α may involve inhibition of the PI3K/Akt pathway, although this may not be the complete story. On this basis, a better understanding of the mechanism of hypoxia-induced retinal angiogenesis may pave the way for the design of therapeutic approaches to treat and prevent aberrant retinal response to hypoxic injury.

References

1 Zaher TE, Miller EJ, Morrow DM, et al: Hyperoxia-induced signal transduction pathways in pulmonary epithelial cells. Free Radic Biol Med 2007;42:897–908.
2 Rojas A, Figueroa H, Re L, et al: Oxidative stress at the vascular wall. Mechanistic and pharmacological aspects. Arch Med Res 2006;37:436–448.
3 Shweiki D, Itin A, Soffer D, Keshet E: Vascular endothelial growth factor induced by hypoxia may mediate hypoxia-initiated angiogenesis. Nature 1992;359:843–845.
4 Kaur C, Sivakumar V, Foulds WS: Early response of neurons and glial cells to hypoxia in the retina. Invest Ophthalmol Vis Sci 2006;47:1126–1141.
5 Wang GL, Semenza GL: Characterization of hypoxia-inducible factor 1 and regulation of DNA binding activity by hypoxia. J Biol Chem 1993;268:21513–21518.
6 Jung F, Palmer LA, Zhou N, Johns RA: Hypoxic regulation of inducible nitric oxide synthase via hypoxia inducible factor-1 in cardiac myocytes. Circ Res 2000;86:319–325.
7 Toda N, Nakanishi-Toda M: Nitric oxide: ocular blood flow, glaucoma, and diabetic retinopathy. Prog Retin Eye Res 2007;26:205–238.
8 Baek SJ, Eling TE: Changes in gene expression contribute to cancer prevention by COX inhibitors. Prog Lipid Res 2006;45:1–16.
9 Smith LE, Wesolowski E, McLellan A, Kostyk SK, D'Amato R, Sullivan R, D'Amore PA: Oxygen-induced retinopathy in the mouse. Invest Ophthalmol Vis Sci 1994;35:101–111.
10 Nejadkey F, Nahavandi A, Dehpour AR, Mani AR: Role of nitric oxide in the gastroprotective effect of lithium. Pathophysiology 2006 May;13:85–89.
11 Hung CR: Role of gastric oxidative stress and nitric oxide in formation of hemorrhagic erosion in rats with ischemic brain. World J Gastroenterol 2006;12:574–581.
12 Barocelli E, Ballabeni V, Ghizzardi P, Cattaruzza F, Bertoni S, Lagrasta CA, Impicciatore M: The selective inhibition of inducible nitric oxide synthase prevents intestinal ischemia-reperfusion injury in mice. Nitric Oxide 2006;14:212–218.
13 Morita M, Ohneda O, Yamashita T, Takahashi S, Suzuki N, Nakajima O, Kawauchi S, Ema M, Shibahara S, Udono T, Tomita K, Tamai M, Sogawa K, Yamamoto M, Fujii-Kuriyama Y: HLF/HIF-2α is a key factor in retinopathy of prematurity in association with erythropoietin. EMBO J 2003;22:1134–1146.
14 Brafman A, Mett I, Shafir M, Gottlieb H, Damari G, Gozlan-Kelner S, Vishnevskia-Dai V, Skaliter R, Einat P, Faerman A, Feinstein E, Shoshani T: Inhibition of oxygen-induced retinopathy in RTP801-deficient mice. Invest Ophthalmol Vis Sci 2004;45:3796–3805.
15 Natarajan R, Jones DG, Fisher BJ, Wallace TJ, Ghosh S, Fowler AA 3rd: Hypoxia inducible factor-1:regulation by nitric oxide in posthypoxic microvascular endothelium. Biochem Cell Biol 2005;83:597–607.
16 Wang FS, Kuo YR, Wang CJ, Yang KD, Chang PR, Huang YT, Huang HC, Sun YC, Yang YJ, Chen YJ: Nitric oxide mediates ultrasound-induced hypoxia-inducible factor-1alpha activation and vascular endothelial growth factor-A expression in human osteoblasts. Bone 2004;35:114–123.

17 Mateo J, Garcia-Lecea M, Cadenas S, Hernandez C, Moncada S: Regulation of hypoxia-inducible factor-1α by nitric oxide through mitochondria-dependent and -independent pathways. Biochem J 2003;376:537–544.
18 Yin JH, Yang DI, Ku G, Hsu CY: iNOS expression inhibits hypoxia-inducible factor-1 activity. Biochem Biophys Res Commun 2000;2791:30–34.
19 Lu DY, Liou HC, Tang CH, Fu WM: Hypoxia-induced iNOS expression in microglia is regulated by the PI3-kinase/Akt/mTOR signaling pathway and activation of hypoxia inducible factor-1α. Biochem Pharmacol 2006; 72:992–1000.
20 Pore N, Jiang Z, Shu HK, Bernhard E, Kao GD, Maity A: Akt1 activation can augment hypoxia-inducible factor-1α expression by increasing protein translation through a mammalian target of rapamycin-independent pathway. Mol Cancer Res 2006;4:471–479.
21 Ardyanto TD, Osaki M, Tokuyasu N, Nagahama Y, Ito H: CoCl2-induced HIF-1α expression correlates with proliferation and apoptosis in MKN-1 cells: a possible role for the PI3K/Akt pathway. Int J Oncol 2006;29: 549–555.
22 Kazi AA, Koos RD: Estrogen-induced activation of hypoxia-inducible factor-1α, vascular endothelial growth factor expression, and edema in the uterus are mediated by the phosphatidylinositol 3-kinase/Akt pathway. Endocrinology 2007;148:2363–2374.